LETTER TO THE EDITOR

Mutual amplification of sensory nerve outgrowth and tumor progression in myeloma

Authors

Motosumi Nakagawa,[1] Masahiro Hiasa,[1] Jumpei Teramachi,[2] Takeshi Harada,[3] Asuka Oda,[3] Go Nishino,[1] SooHa Matsuki,[1] Mariko Hanawa,[1] Ariunzaya Bat-Erdene,[4] Takako Taniguchi,[5] Hisaaki Taniguchi,[5] Koichi Tsuneyama,[6] Tatsuya Tominaga,[7] Eiji Tanaka,[1] Takeshi Y. Hiyama,[8] Ken-ichi Matsuoka,[3] Yoshio Katayama[9] and Masahiro Abe[10]

[1]Department of Orthodontics and Dentofacial Orthopedics, Tokushima University Graduate School of Biomedical Sciences, Tokushima, Japan; [2]Department of Oral Function and Anatomy, Faculty of Medicine, Dentistry and Pharmaceutical Sciences, Okayama University Graduate School, Okayama, Japan; [3]Department of Hematology, Endocrinology and Metabolism, Tokushima University Graduate School of Biomedical Sciences, Tokushima, Japan; [4]Department of Immunology, School of Bio-Medicine, Mongolian National University of Medical Sciences; and Department of Health Research, Graduate School of Mongolian National University of Medical Sciences, Ulaanbaatar, Mongolia; [5]Division of Disease Proteomics, Institute for Enzyme Research, University of Tokushima, Tokushima, Japan; [6]Department of Pathology and Laboratory Medicine, Tokushima University Graduate School of Biomedical Sciences, Tokushima, Japan; [7]Department of Bioanalytical Technology, Tokushima University Graduate School of Biomedical Sciences, Tokushima, Japan; [8]Department of Integrative Physiology, Tottori University Graduate School and Faculty of Medicine, Tottori University, Tottori, Japan; [9]Hematology, Kobe University Hospital, Kobe, Japan and [10]Department of Hematology, Kawashima Hospital, Tokushima, Japan.

Correspondence:
M. HIASA - mhiasa@tokushima-u.ac.jp
J. TERAMACHI - jumptera@okayama-u.ac.jp

https://doi.org/10.3324/haematol.2025.300309

Received: November 27, 2025.
Accepted: February 18, 2026.
Early view: February 26, 2026.

©2026 Ferrata Storti Foundation
Published under a CC BY-NC license

Supplementary Figure 1

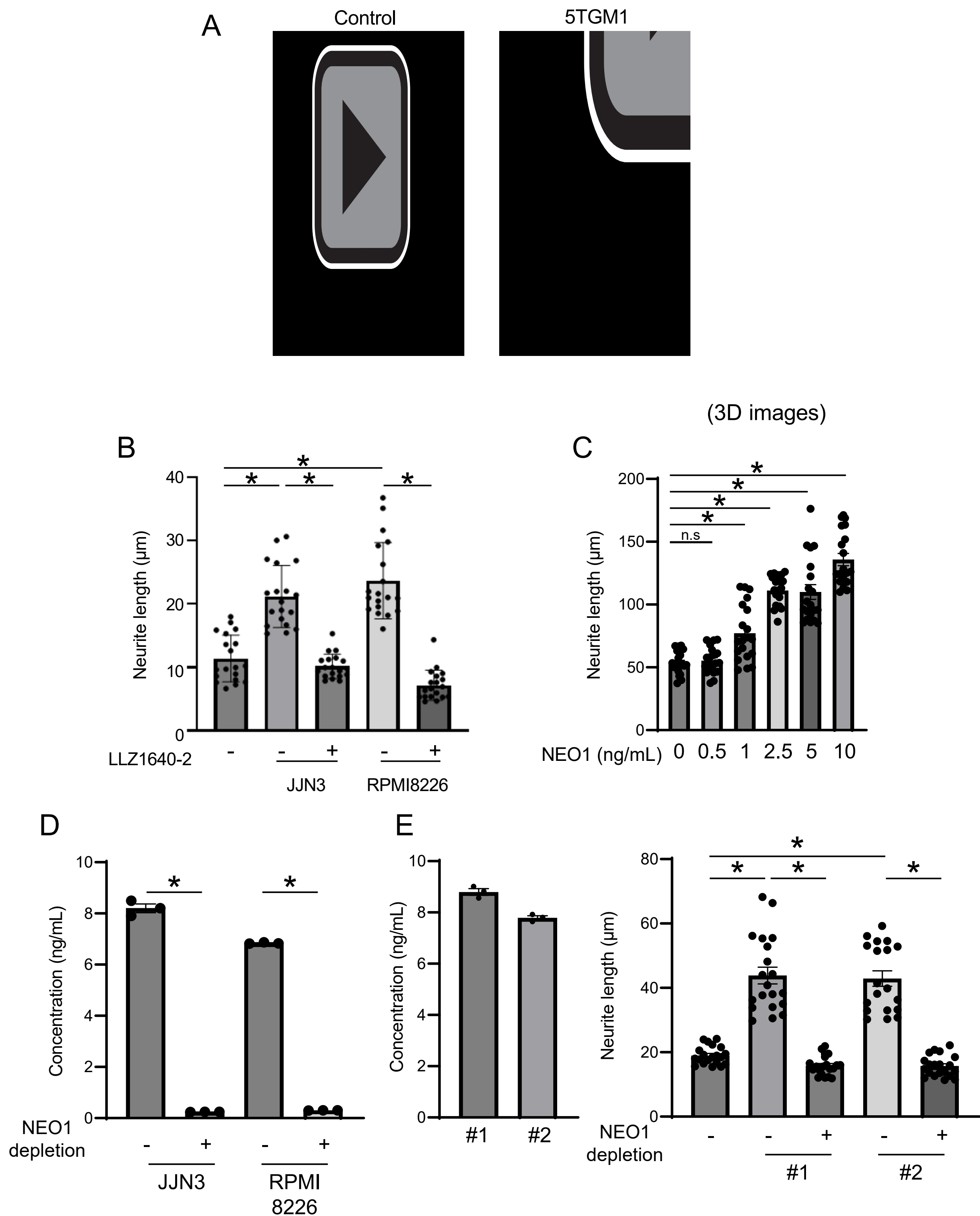

Supplementary Figure 1.

(A) 5TGM1 MM cells were inoculated into tibiae in right hind legs of SCID mice. Tumor bearing tibia (right) and intact one (left) as a control were resected from the same mice at 4 weeks after the inoculation, and subjected to optical clearing with the CUBIC method. CGRP-positive SNs were visualized by a light sheet microscope. Images were displayed in three dimensions. (B) JJN3 and RPMI8226 MM cells were treated for 24 hours in the presence or absence of the TAK1 inhibitor LLZ1640-2 at 5 μM. After washing to remove LLZ1640-2, viable cell numbers were counted, and the viable cells were cultured at $5x10^5$/mL. After culturing for 2 days, their culture supernatants were harvested. The culture supernatants were added at 20% to the neural cell line Neuro2a in the presence of NGF at 10 ng/mL. The length of the longest neurite from each cell were measured using NeuronJ. Data are expressed as mean ± SD. *$P<0.05$. (C) Recombinant NEO1 was added at the indicated concentrations to the neural cell line Neuro2a in the presence of NGF at 10 ng/mL. After culturing for 7 days, the length of the longest neurite from each cell was measured using NeuronJ. (D) Concentrations of

NEO1 in pre- and post-depletion supernatants were measured by ELISA. (E) Concentrations of NEO1 in culture supernatants of primary $CD138^{+}$MM cells from patients with MM were measured by ELISA (left). The conditioned media with or without the immunodepletion of NEO1 were added at 20% to Neuro2a in the presence of NGF at 10 ng/mL (right). After culturing for 2 days, the length of the longest neurites from each cell were measured using NeuronJ.

Supplementary Figure 2

F

Protein name	Relative abundance (ratios of MS intensity vs PBMC (log2))					Change by TAK1 inhibition (MS intensity ratio (log2))			
	PBMC	INA6	KMS11	RPMI8226	U226B1	INA6	KMS11	RPMI8226	U226B1
Neogenin1	-0.066	4.644	4.674	5.145	6.887	-1.227	-0.560	-1.390	-1.692
Cyclin-dependent kinases regulatory subunit 1	-0.311	3.174	5.062	4.717	4.489	-0.188	-0.726	-0.255	-0.549
Neuroserpin1	-0.146	3.978	1.646	3.955	2.378	-3.542	-4.002	-0.007	-3.020
ADAM9	-0.051	1.507	1.664	3.801	1.942	-3.053	-3.100	-2.663	-3.728
V-type proton ATPase subunit S1	-0.024	2.234	2.332	4.633	2.749	-3.606	-3.560	-2.025	-3.317
Alpha-galactosidase A	-0.042	1.623	2.072	5.163	1.737	-1.824	-3.963	-1.393	-0.634
Glucosylceramidase	-0.046	1.997	2.498	4.936	1.027	-3.261	-3.989	-2.108	-3.911
Palmitoyl-protein thioesterase 1	-0.107	4.189	3.890	5.499	3.618	-2.121	-2.246	-1.164	-1.906
Hydroxymethylglutaryl-CoA synthase	-0.117	3.588	3.976	6.311	4.185	-3.915	-0.157	-0.307	-1.003
Stromal cell-derived factor 2	-0.045	0.313	2.728	2.528	2.595	0.392	-0.253	-3.844	-1.092
Beta-galactosidase	-0.092	0.871	0.574	2.550	2.204	-0.050	0.503	-0.314	-2.244

Supplementary Figure 2.

MM cell-specific, TAK1-dependent proteins were selected by a comprehensive secretome analysis for culture supernatants. The indicated MM cell lines and peripheral blood mononuclear cells (PBMC) were cultured in serum-free medium ($5x10^5$ cells/mL) in the presence or absence of the TAK1 inhibitor LLZ1640-2 at 0.625-10 µM for 24 hours. Their conditioned media were then centrifuged (15,000 rpm, 15 minutes, 4°C) and filtered using a 0.2 µm membrane filter. The secreted proteins were cleaned up by chloroform/methanol, suspended in 10 mM Hepes buffer (pH 8.9) containing 6M urea/2M thiourea and digested with Lys-C protease. The samples were further digested with trypsin as described previously. Each 1 mg digested protein was subjected to mass spectrometry (MS) using an Orbitrap Fusion Tribrid Mass Spectrometer (Thermo Fisher Scientific) in a data-dependent acquisition mode as described previously. The MS data obtained were processed with MaxQuant software (ver. 1.5.3.30), and Andromeda search engine was used to search the UniProt KB FASTA database (20,195 reviewed entries, Ver. from April 2017). (A) VennDiagram of proteins secreted from MM cell lines and PBMC. The numbers of proteins detected are shown in parentheses. Proteins detected in all 4 MM cell lines but not in that of PBMC were circled (202 proteins). (B) Cluster analysis of proteins secreted from 4 MM cell lines and the effects of the TAK1 inhibitor LLZ1640-2 on the secretome. Only proteins showing significant increase (LFQ ≧2 reported from MaxQuant software) in the secretome of 4 MM cell lines compared to that of PBMC were selected in the analysis (750 proteins, right panel). The effect of the TAK1 inhibition on secretion levels of those proteins were analyzed in the secretome of four MM cell lines (left panel). Data from 4 independent measurements were used for the clustering individually, and signals that were originally zero were imputed with random numbers from a normal distribution. Heat map analysis and hierarchical clustering (Manhattan distance) were performed using MultiExperiment Viewer (MeV software version 4.9, https://mev.tm4.org/#/welcome). (C) Cluster 9 contains proteins with high basal secretion levels in all of the 4 MM cell lines showing a decrease upon the LLZ1640-2 addition. Neogenin1 was detected in the cluster 9, and marked with an asterisk. (D) We also performed K-means clustering analysis of proteins secreted from four MM cell lines showing significant effects of TAK1 inhibition on the secretome. Secreted proteins from four MM cell lines were cultured with varying concentrations of LLZ1640-2. Total 2,872 proteins were identified with ≧2 RazorUnique peptides reported from MaxQuant. Of these 2,411 proteins were quantified with LFQ ≧2 reported from MaxQuant software). Signals that were originally zero were imputed with random numbers from a normal distribution. After imputation, the quantitation values were evaluated with one-way ANOVA, and total 1,533 proteins with significance ($p<0.05$) were selected for clustering. (E) K-means clustering analysis of proteins secreted from four MM cell lines showing significant effects of the TAK1 inhibition on the secretome. The proteomics data files are available on request from the corresponding authors. (F) The selected proteins are listed according to high basal secretion and TAK1 dependency. Average ratios of abundance of basal secretion and fold change from their baselines with TAK1 inhibition (10 µM) are tabulated in each MM cell line.

Supplementary Figure 3

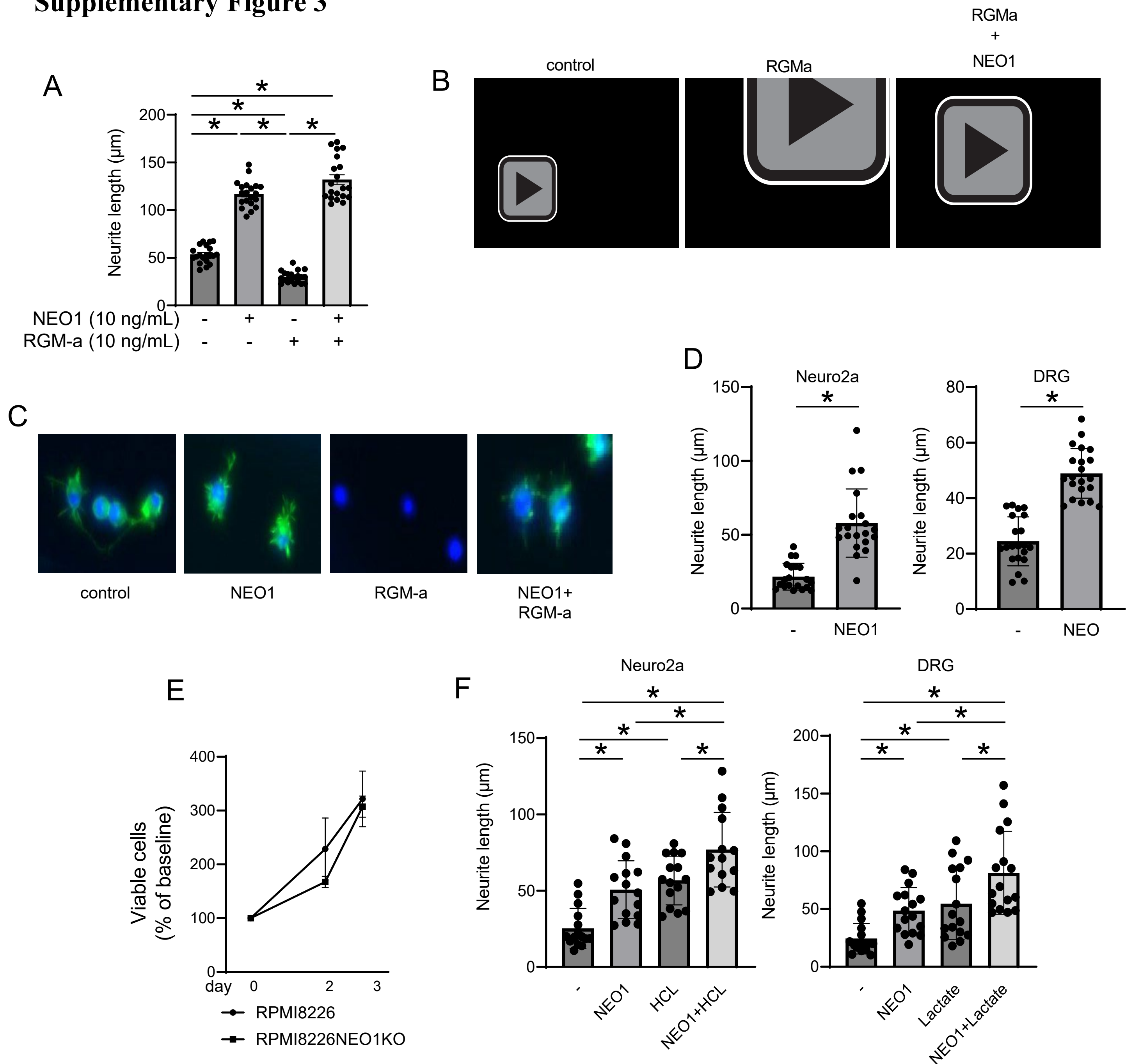

Supplementary Figure 3.
(A) rRGM-a was added at 10 ng/mL to Neuro2a in the presence of NGF at 10 ng/mL. After culturing for 2 days, the length of the longest neurite from each cell was measured using NeuronJ. (B) Neuro2a cells were differentiated into SNs with neurite extension in the presence of NGF at 10 ng/mL. The cells were stained with calcein AM. Recombinant NEO1 (NEO1) or recombinant RGMa (RGMa) at 100 ng/mL alone, or both in combination were added, and neurite contraction was observed over time under a phase-contrast microscope. Time-lapse images were recorded for 2 hours. (C) Actin polymerization (F-actin) was visualized using phalloidin (green). Nuclei were counterstained with DAPI (blue). Representative images are shown. (D) Recombinant NEO1 (100 ng/mL) was added to Neuro2a in the presence of NGF at 10 ng/mL and primary DRG cells under a serum-free condition. After 3 days, the longest neurite of each cell was measured using NeuronJ. (E) *NEO1*-KO and control RPMI8226 cells were cultured at 5×10^4/mL. Variable cell numbers were counted. (F) Neuro2a cells were cultured in 24-well plates for 2 days in the presence of NGF at 10 ng/mL under acidic conditions (pH 6.8) prepared by lactic acid (Sigma-Aldrich) or HCl. Recombinant NEO1 was added at 100 ng/mL as indicated. After 2 days, the longest neurite of each cell was measured using NeuronJ. Data are expressed as mean ± SD. *P<0.05.